# OPTIMIZING ELECTRICAL AND FATIGUE PROPERTIES OF A POLYMER-BASED COMPOSITE HIGH DEFLECTION STRAIN GAUGE

David S Wood, David Fullwood, Anton Bowden Brigham Young University Provo, Utah/ USA

### **ABSTRACT**

Polymer-based composite strain gauges are a quickly expanding technology area that exhibits advantages such as large strain capacity and high sensitivity to changes in strain. These strain gauges use an inert matrix embedded with one or more conductive fillers to exploit the elasticity of the matrix and the electrical conducting properties of the filler materials. However, determining the optimal composition of the filler materials for a particular application can be a challenging and iterative process. In the present work, the composition of a nano-nickel/silicone composite gauge was optimized based on four independent design parameters related to both mechanical and electrical performance of the gauge. Specifically, the critical impedance, critical strain, strain to failure, and initial impedance of the gauges were optimized by varying the weight ratios of Libra Gloss silicone base material, nickel nanostrands, and nickel-coated carbon fibers. The approach leveraged a combination of black-box design space modeling and multi-objective Bayesian optimization algorithm. The data from tensile tests were analyzed and compositions for a new optimal combination of parameters were found. This methodology was used to find transducer compositions that were appropriate for high strain, low-cycle wearable applications in biomechanical measurement.

Keywords: Many-objective optimization, high deflection strain gauge, polymer composite

Corresponding author: Anton Bowden

DOI: (will be filled by SAMPE)

## 1. INTRODUCTION

Characterizing a novel material, regardless of the intended application, can quickly become a process that is expensive in terms of time and/or money. The number of parameters and design objectives to consider can become prohibitively large depending on the complexity and accuracy needed in the models of the material. This work attempts to reduce the time and number of iterations needed to confidently find an optimal composition of a tri-phasic composite by systematically exploring the material's design space efficiently using a multi-objective Bayesian optimization algorithm.

Polymer-based composite strain gauges are desirable for biomechanical measurement applications because of their large strain capacity and their sensitivity to changes in strain [1, 2] . A variety of different composites have been developed [3-17]; the bulk of which use an inert matrix embedded with a conductive filler to exploit the elasticity of the matrix and the electrical conducting properties of the filler material. Currently there is a wide variety of high deflection strain gauges with a vast range of properties. This makes certain strain gauges more useful for

Copyright 2021. Used by the Society of the Advancement of Material and Process Engineering with permission.

different applications. However, one does not necessarily have to use a different strain gauge to find the best sensor for their intended application. Most high deflection strain gauges are a composite material, and, therefore, the proportions of the materials can be altered to elicit a spectrum of mechanical and electrical properties. For example, a higher proportion of electrically conductive filler materials in the composition for a polymer strain gauge might simultaneously enhance the electrical sensitivity for a particular range of strain, decrease the sensitivity for other ranges of strain, increase the overall mechanical stiffness of the gauge, and decrease the strain to failure for the gauge. Thus, a significant challenge in working with this category of sensors is to identify an optimal composition that achieves both the mechanical and electrical properties appropriate to a particular application [18, 19].

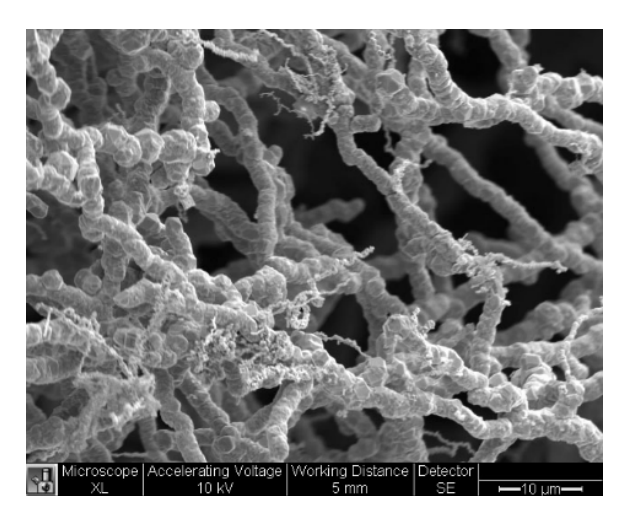


Figure 1. SEM of NiNs

This work looks at a tri-phasic silicone/nickel composite [18, 20-23] and optimizes the proportions of two different nickel filler materials -nickel nanostrands (NiNs; Error! Reference source not found.) and nickel coated carbon fiber (NCCF, Error! Reference source not found.) based on four distinct electrical and mechanical design goals. The composition is iteratively optimized using a combination of black-box design space modeling and a multi-objective Bayesian optimization algorithm.

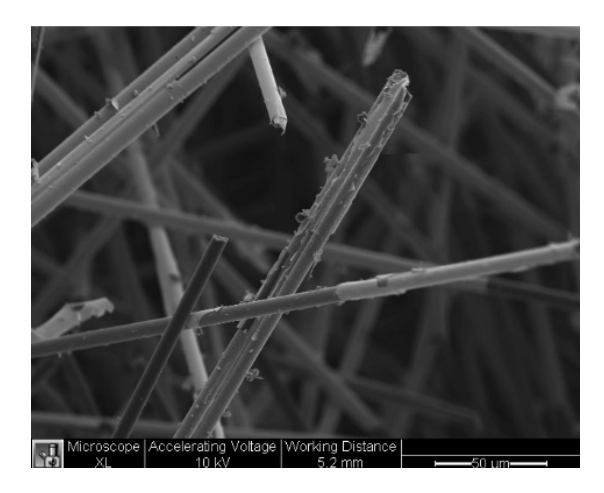


Figure 2. SEM of NCCF

The influence of the composition of a composite made up of a gloss clear silicone from Zodiac (\_\_\_\_\_) matrix with NCCF and NiN filler materials on multiple mechanical/electrical properties are studied. This paper focuses on optimizing parameters using a statistical based approach that simultaneously optimizes multiple design spaces. To match the assumptions made by the multi-objective Bayesian optimization algorithm, no assumptions about the local behavior of the objective spaces are made while estimating the objective functions. Therefore, a local surface estimation is used to develop the Gaussian processes used in the optimization. This work aims to optimize the critical impedance, critical strain, strain to failure, and initial impedance for a specific formulation of a polymer-based high-deflection strain gauge using a multi-objective Bayesian optimization algorithm.

An approach based on Bayesian multi-objective optimization is flexible enough to take many inputs and create a Pareto front of solutions for numerous objective functions where there is no prior analytical knowledge of the objective spaces; this allows researchers to take a black-box approach that requires less objective space samplings than a grid search approach [24]. Objective functions in Bayesian multi-objective optimization may also be multimodal or non-convex [25, 26]; no assumptions about the curvature of the objective spaces are made.

## 2. EXPERIMENTATION

Data from tensile tests are analyzed and compositions for an optimal combination of parameters are found using a Bayesian multi-objective optimization approach. This approach is flexible enough to take many inputs and create a Pareto front of solutions for numerous objective functions where there is no prior knowledge analytical knowledge. Objective functions in Bayesian multi-objective optimization may also be multimodal or non-convex.

# 2.1 Making Samples

High-deflection strain gauges were made by mixing the requisite amount of NCCF and surfactant with the silicone. The NCCF were screened and mixed with a surfactant to increase their incorporation into the silicone. NiNs and catalyst were finally added to the mixture before forming the samples in an aluminum mold. The mold is vacuum sealed and the composite mixture is cured for 1 hour and 20 minutes at 74° C. To eliminate variation caused by different people

manufacturing the sensors, all sensors were manufactured by one individual throughout the study. Because nothing was known a priori about the objective functions, a pseudo-random set of five compositions was used to seed the optimization algorithm. These compositions were determined using Latin hypercube sampling

# 2.2 Testing Samples

For each test, a sample was mounted into an Instron 3340 Series single column tensile tester (Norwood, Massachusetts, USA) using a 500 N load cell and clamps with copper leads connecting the sensor into a voltage divider, seen in **Error! Reference source not found.** The sensor was electrically isolated from the metallic tester by covering the clamp faces with a natural rubber padding prior to testing. The circuit was excited with a 1-volt square wave at 50 Hz. The voltage source and measurement tool were provided through an Analog Discovery (Agilent, Inc., Pullman, Washington, USA). The voltage drop across the sample was sampled at 1000 Hz with a DAQ 9171 (Texas Instruments, Dallas, Texas, USA). Displacement data was recorded by the Intron tensile tester sampling at 10 Hz. A minimum of five sensors of each composition were tested. Sensors were stretched to mechanical failure at a constant 4.23 mm/s.



Figure 3. Experimental set up

Data was then collected from the resulting electrical impedance versus mechanical strain plot of the test. Four data points were taken from each plot: initial impedance, ultimate strain, critical impedance, and critical strain. The critical impedance was defined as the characteristic peak in impedance of the impedance vs strain curve at low strains before the impedance decreased linearly (Figure 4a). The critical strain was defined as the strain at which the critical impedance occurs (Figure 4b). For this composite sensor, the initial impedance, critical impedance and strain to failure are to be maximized, and the critical strain is to be minimized.

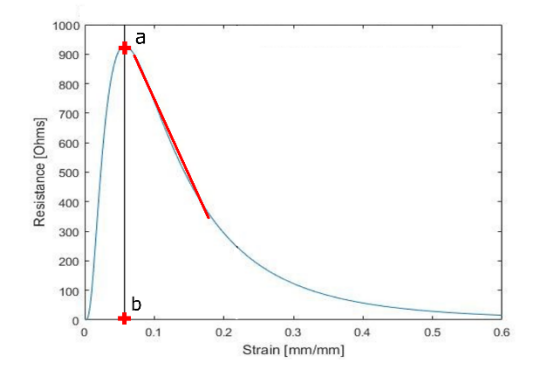


Figure 4. Electrical impedance versus mechanical strain of strain gauge

# 2.3 Bayesian Optimization

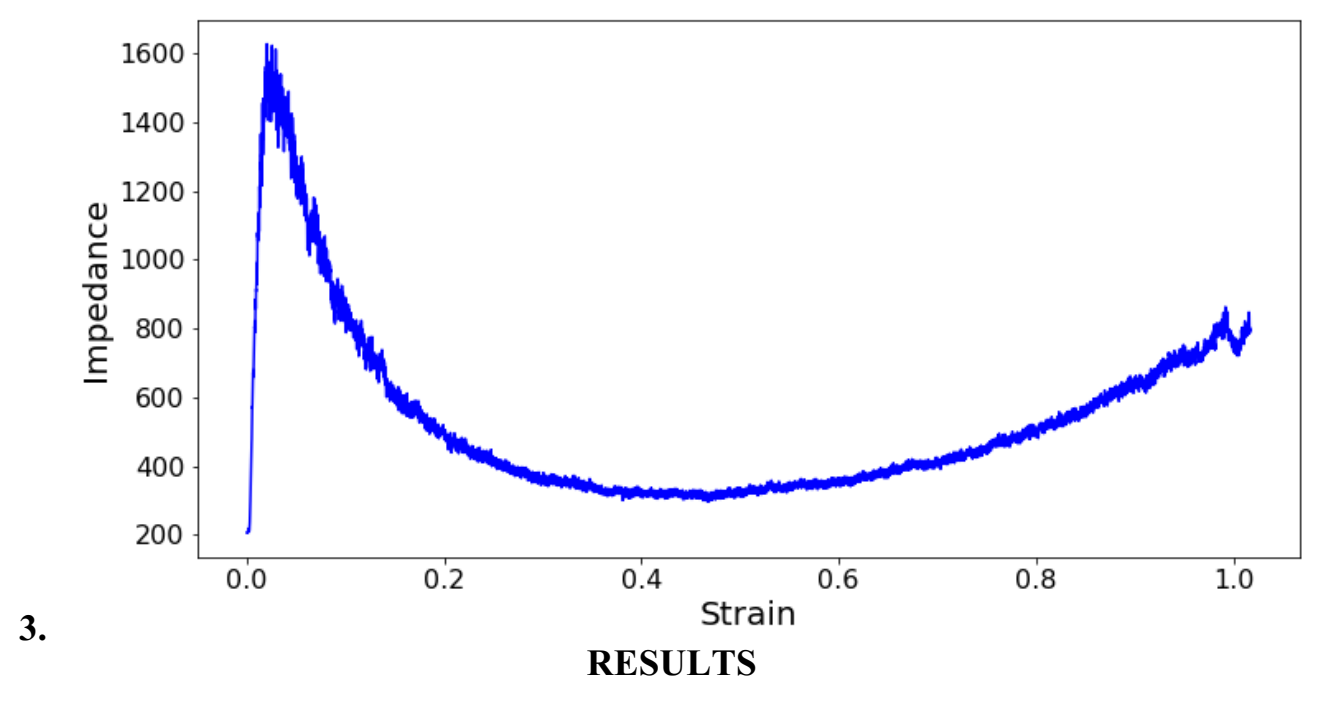
The optimization process fit a surface to each parameter of interest separately and used a multiobjective Bayesian optimization algorithm to estimate a 4-dimensional Pareto front of candidates for a new optimal composition. Each objective function was fit with a multivariate polynomial as a function of the weight percentages of NiNs and NCCF using Scikit-Learn (more info). A pipeline consisting of Scikit-Learn's PolynomialFeatures, StandardScaler, and LinearRegression functions created and stored the models. Four objective function polynomials were then optimized using a Bayesian approach based on the Python class MOBOpt [27]. The algorithm maximizes the objective functions, therefore objective functions that were to be minimized were negated beforehand. This approach optimized surrogate functions instead of the true objective functions with a genetic algorithm, which greatly decreased the requisite number of objective function calls in the algorithm. The optimization algorithm used an expected hypervolume improvement metric in NGSA-II to find the Pareto front of a population of 100 members. NSGA-II uses an elitism based on non-dominated sorting method for ranking and sorting each individual. Also uses a crowding distance approach in its section operator for keeping the diversity among the obtained Pareto optimal solutionsThe surrogate functions used in the actual optimization were Gaussian processes. These sets of functions are exact distributions over functions that were characterized by their mean and covariance functions [28]. In other words, they were functions that returned the mean and variance of the Gaussian distribution of the function at any point in the design space. The Matern kernel was used in the Gaussian processes choosing v = 1.5.

Because the objective functions were iteratively approximated, this process quickly found an optimum while accurately estimating the curvature of the different objective spaces with polynomial approximations. Balancing exploration and exploitation, this approach increased the confidence of finding a true, global maximum while avoiding local maxima.

In each iteration, researchers chose one to three compositions from the Pareto front to test and included its data in the next iteration in the optimization process. One composition was selected if the Pareto front was continuous and centered around one location in the design space. Additional compositions were selected if the Pareto front in the design space is noncontinuous. A constrained optimization technique was used to bound the search area to the ranges of weight percentages of NiNs and NCCF that had been previously tested. Compositions outside of these bounds have been experimentally found to result in gauges that produce no electrical output or are too brittle to use as strain gauges.

Figure 5. Representative impedance versus strain plot

In each iteration, the genetic algorithm ran for 250 iterations. Due to the construction of the MOBOpt class, a convergence criterion is not required but a higher number of iterations is needed to ensure adequate convergence of the majority of the population. The algorithm's convergence criterion is as follows: once the design space of the Pareto front consists entirely of compositions that have been tested an optimum has been found.



A total of 7 iterations were necessary for the Pareto front to meet the convergence criterion. A total of 21 different compositions were tested; this includes the four seeding compositions to start the algorithm and 16 additional compositions. The process included five noncontinuous Pareto fronts that were sampled multiple times. Iterations and 7 resulted in continuous Pareto fronts that required one sample. These two fronts were also localized to one composition with little variance within the population. In each iteration, the Pareto front consisted of the entire 100 member population after the 250 iterations were performed.

**Error! Reference source not found.** shows the initial objective spaces after the seeding compositions were tested. The algorithm systematically explored the design space for the first 4 iterations and approximated the optimal value for the remaining two iterations. Each objective function adequately described with a 2-degree polynomial. The curve fit was fitted with the lowest degree polynomial where the RMSE no longer decreased. All subsequent iterations were fitted in the same fashion. Five out of the seven iterations resulted in a noncontinuous Pareto front that was sampled in multiple locations.

The final objective functions are shown in Figure 7. All objectives were fitted with a 5-degree polynomial. Three additional compositions were tested after finding the optimal value to ensure the curve fitted objective functions' accuracy across the design space.

It was found that by optimizing the objective functions in 7 iterations, the parameters of interest were changed by the amounts shown in Error! Reference source not found. Each of the four parameters of interest improve from the initial seeding compositions. With the additional compositions used to fit the models, the expected values from the model accurately predicted the experimental averages. The final models of the four objectives predicted the initial impedance, strain to failure, critical impedance, and critical strain as 769 Ohms, 0.794, 10239 Ohms, 0.0428, respectively. The error of the models' for the initial impedance, strain to failure, critical impedance, and critical strain were 211%, 23%, 221%, 30%, respectively. The initial impedance improved an average of over the 7 iterations. The strain to failure increased by %, the critical impedance increased by %, and the critical strain decreased by %.

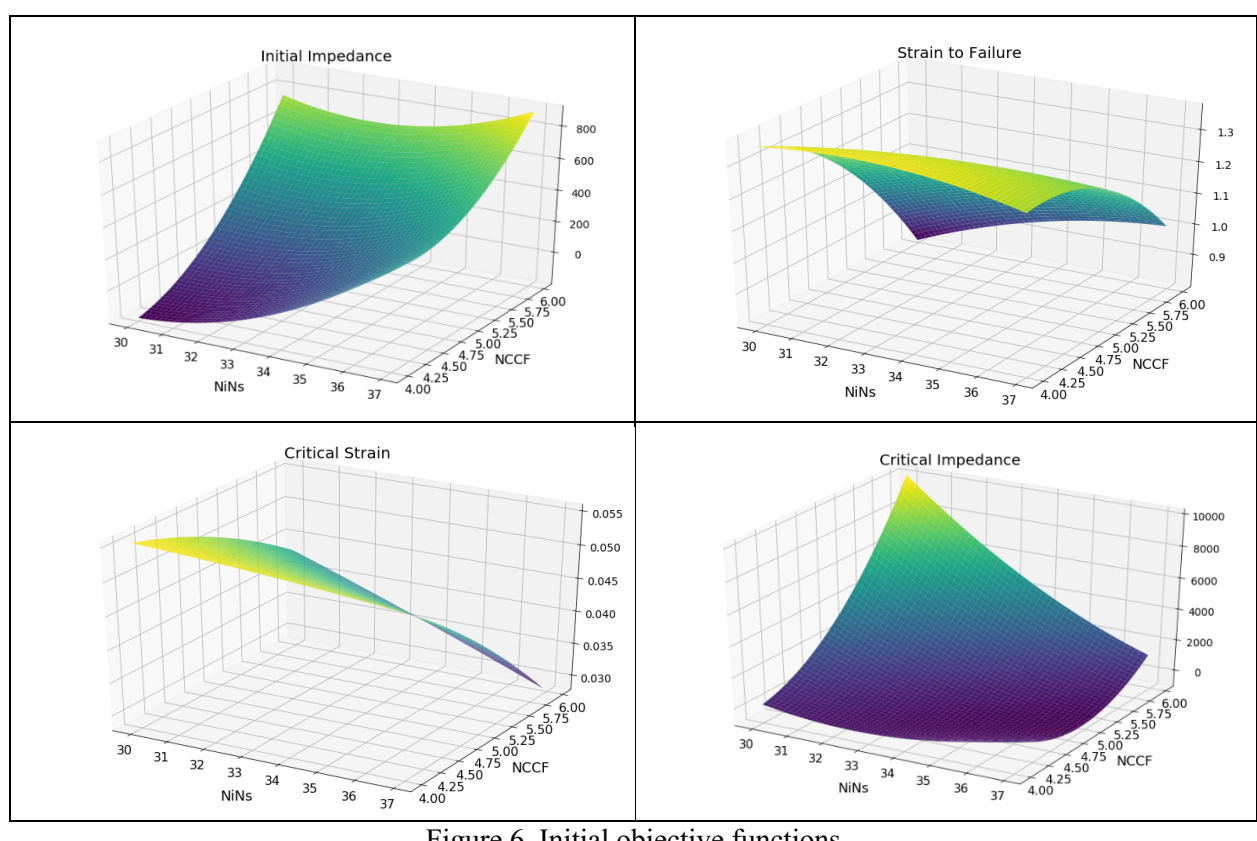


Figure 6. Initial objective functions

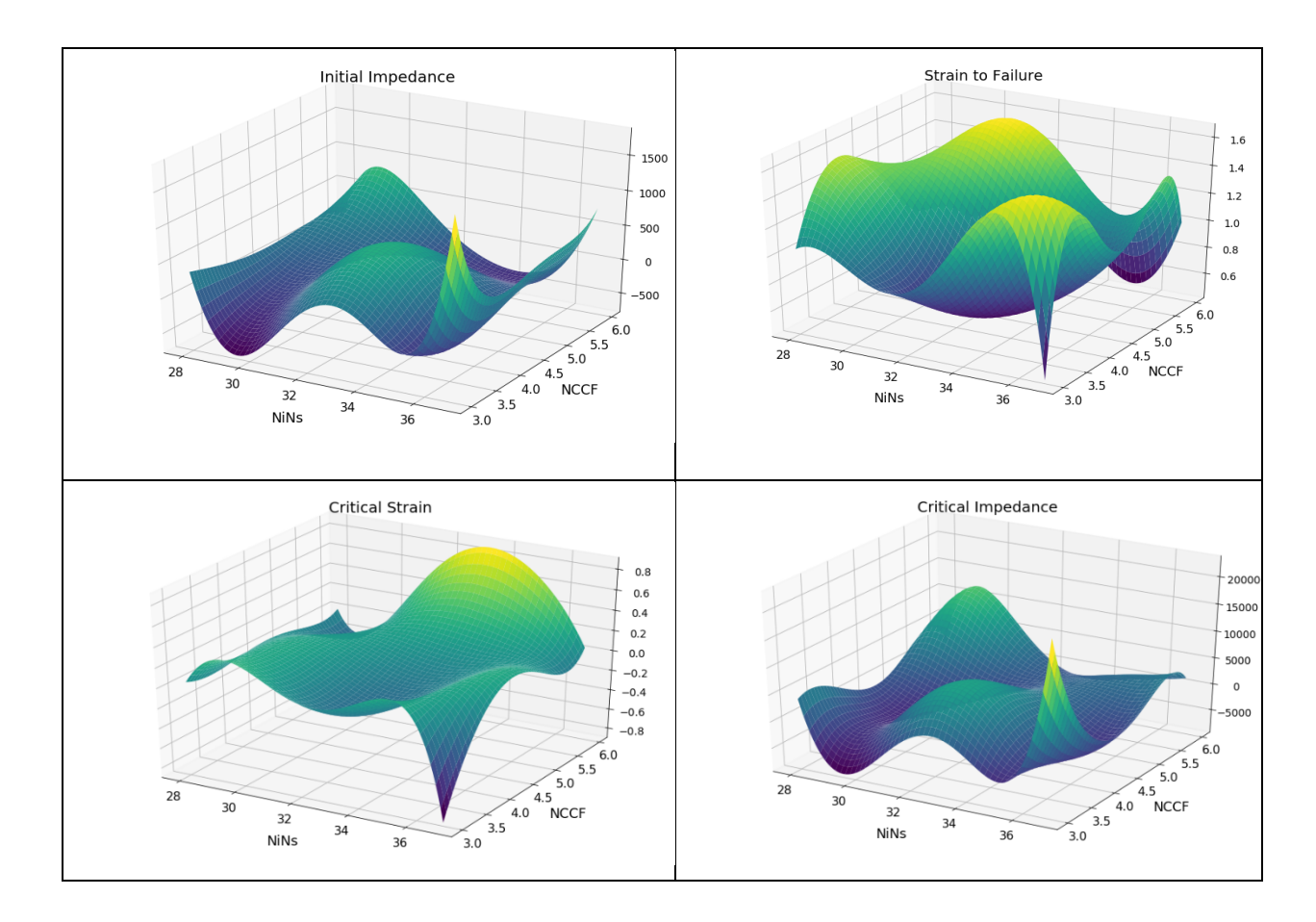


Figure 7. Final objective spaces

## 4. CONCLUSIONS

The optimum that was found adequately found values near the extrema of each objective function. The final value of the initial impedance was, from the shape of the final curve fit of the initial impedance's objective function, a local maximum whereas the failure strain and critical impedance settled near the predicted global maximum. The critical strain, which was the only objective to be minimized, settled near the bottom of the lowest valley in the design space. The final state of the objective space models are mostly intuitive while some predictions will contain some error. For example, a sensor with 7% NiNs, and 37% NCCF intuitively will not have a high initial impedance yet the model predicts otherwise. Intuitively, more conductive filler material should result in a sensor with lower impedances because there is more material to help conduct a current. This shows that the model is still imperfect, but the aim of this work is to quickly determine an optimum with as few direct samplings (i.e. making and testing sensors) of the objective functions as possible by optimizing Gaussian processes of the fitted objective spaces. This means the final fitted models will contain some errors in their predictions; however, researchers can be confident in their solution. Further testing of the design space confirmed that the predicted initial impedance at this composition was incorrect.

Once the algorithm determined an optimal composition, three additional compositions were tested in areas that were not searched during the optimization process to ensure that the model accurately predicts those areas of the design space as well. The models did not change at the extrema as a result of these additional data. The additional data, however, strengthened the conclusions of the optimization process: a true global optimum was found using the algorithm outlined in this work.

Composition			Initial	Critical	Critical	Ultimate
NiNs wt%	NCCF		Impedance	Impedance	Strain	Strain
	wt%					
35	4	Initial	77	249	0.055	0.83
37	4	Initial	432	1127	0.052	1.30
33	5	Initial	163	588	0.046	1.22
30	6	Initial/Final	247	3194	0.033	1.03

Table 1. Results of optimization experiment

This procedure may save researchers valuable time due to the limited number of iterations and total number of compositions that were required to find the optimal composition. If a grid search approach was taken over the bounded design space (28-37 wt% NiNs, and 3-7 wt% NCCF) a total of 36 compositions would have to be tested for a resolution of 1.0 wt% in each parameter. With a resolution of 0.5 wt%, a total of 72 compositions would have to be tested. Compared to these two approaches, the multi-objective Bayesian optimization approach found an optimal value faster and with greater accuracy. If a grid of 1.0 wt% resolution is used, the researcher cannot confidently assume that the true optimal value lies on a point in the grid. Thus, additional compositions around the best candidate solution would have to be tested to ensure the true optimum is found. The multi-objective Bayesian optimization approach uses the objective functions as continua and thus inherently has a finer resolution over a grid search approach.

A few limitations are noted for this study. Variance between sensors may be due to a nonuniform dispersion of nanoparticles either before or after deposition of the composite material. NCCF was seen to form into hardened balls if not sufficiently screened.

A study of the influence of an electrically conductive polymer composite's filler material on its performance was conducted. It was found that by optimizing the objective functions in 7 iterations, the parameters of interest were changed by the amounts shown in **Error! Reference source not found.**. Several objectives pertaining to the mechanical and electrical properties of this high-deflection strain gauge were sufficiently optimized despite each objective space model being complex.

# 5. REFERENCES

1. Lu Y., Biswas, M. C., Guo, Z., Jeon, J. W., & Wujcik, E. K. "Recent Developments in Bio-Monitoring Via Advanced Polymer Nanocomposite-Based Wearable Strain Sensors." *Biosens Bioelectron*. 123(2019): 167-177.

- 2. Yee M. J., Mubarak, N. M., Abdullah, E. C., Khalid, M., Walvekar, R., Karri, R. R., Nizamuddin, S., & Numan, A. "Carbon Nanomaterials Based Films for Strain Sensing Application—a Review." *Nano-Structures & Nano-Objects.* 18(2019).
- 3. Amjadi M., Kyung, K.-U., Park, I., & Sitti, M. "Stretchable, Skin-Mountable, and Wearable Strain Sensors and Their Potential Applications: A Review." *Advanced Functional Materials*. 26(2016): 1678-1698.
- 4. Gong S., Lai, D. T., Wang, Y., Yap, L. W., Si, K. J., Shi, Q., Jason, N. N., Sridhar, T., Uddin, H., & Cheng, W. "Tattoolike Polyaniline Microparticle-Doped Gold Nanowire Patches as Highly Durable Wearable Sensors." *ACS Appl Mater Interfaces.* 7(2015): 19700-8.
- 5. Jeong Y. R., Park, H., Jin, S. W., Hong, S. Y., Lee, S.-S., & Ha, J. S. "Highly Stretchable and Sensitive Strain Sensors Using Fragmentized Graphene Foam." *Advanced Functional Materials*. 25(2015): 4228-4236.
- 6. Xiao X., Yuan, L., Zhong, J., Ding, T., Liu, Y., Cai, Z., Rong, Y., Han, H., Zhou, J., & Wang, Z. L. "High-Strain Sensors Based on Zno Nanowire/Polystyrene Hybridized Flexible Films." *Adv Mater.* 23(2011): 5440-4.
- 7. Chossat J.-B., Park, Y.-L., Wood, R. J., & Duchaine, V. "A Soft Strain Sensor Based on Ionic and Metal Liquids." *IEEE Sensors Journal*. 13(2013): 3405-3414.
- 8. Gullapalli H., Vemuru, V. S., Kumar, A., Botello-Mendez, A., Vajtai, R., Terrones, M., Nagarajaiah, S., & Ajayan, P. M. "Flexible Piezoelectric Zno-Paper Nanocomposite Strain Sensor." *Small.* 6(2010): 1641-6.
- 9. Carvalho Fernandes D. C., Lynch, D., & Berry, V. "3d-Printed Graphene/Polymer Structures for Electron-Tunneling Based Devices." *Sci Rep.* 10(2020): 11373.
- 10. Coppola B., Di Maio, L., Incarnato, L., & Tulliani, J. M. "Preparation and Characterization of Polypropylene/Carbon Nanotubes (Pp/Cnts) Nanocomposites as Potential Strain Gauges for Structural Health Monitoring." *Nanomaterials (Basel)*. 10(2020).
- 11. Dal Lago E., Cagnin, E., Boaretti, C., Roso, M., Lorenzetti, A., & Modesti, M. "Influence of Different Carbon-Based Fillers on Electrical and Mechanical Properties of a Pc/Abs Blend." *Polymers (Basel)*. 12(2019).
- 12. Dios J. R., Garcia-Astrain, C., Costa, P., Viana, J. C., & Lanceros-Mendez, S. "Carbonaceous Filler Type and Content Dependence of the Physical-Chemical and Electromechanical Properties of Thermoplastic Elastomer Polymer Composites." *Materials (Basel)*. 12(2019).
- 13. Du J., Wang, L., Shi, Y., Zhang, F., Hu, S., Liu, P., Li, A., & Chen, J. "Optimized Cnt-Pdms Flexible Composite for Attachable Health-Care Device." *Sensors (Basel)*. 20(2020).
- 14. Hur O. N., Ha, J. H., & Park, S. H. "Strainsensing Properties of Multiwalled Carbon Nanotube/Polydimethylsiloxane Composites with Different Aspect Ratio and Filler Contents." *Materials (Basel)*. 13(2020).
- 15. Ke K., Wang, Y., Li, Y., Yang, J., Potschke, P., & Voit, B. "Nuomici-Inspired Universal Strategy for Boosting Piezoresistive Sensitivity and Elasticity of Polymer Nanocomposite-Based Strain Sensors." *ACS Appl Mater Interfaces.* 11(2019): 35362-35370.
- 16. Sang Z., Ke, K., & Manas-Zloczower, I. "Interface Design Strategy for the Fabrication of Highly Stretchable Strain Sensors." *ACS Appl Mater Interfaces*. 10(2018): 36483-36492.
- 17. Sekertekin Y., Bozyel, I., & Gokcen, D. "A Flexible and Low-Cost Tactile Sensor Produced by Screen Printing of Carbon Black/Pva Composite on Cellulose Paper." *Sensors (Basel)*. 20(2020).
- 18. Baradov D. A., Composition Based Modaling of Silicone Nano- Composite Strain Gauges. 2015.
- 19. David Remington T., & David, T., Biomechanical Applications and Modeling of Quantum Nano-Composite Strain Gauges. 2014.
- 20. David Remington T., & David, T. "Biomechanical Applications and Modeling of Quantum Nano-Composite Strain Gauges." (2014).
- 21. Johnson O. K., Gardner, C. J., Seegmiller, D. B., Mara, N. A., Dattelbaum, A. M., Rae, P. J., Kaschner, G. C., Mason, T. A., Fullwood, D. T., & Hansen, G. "Multiscale Model for the

- Extreme Piezoresistivity in Silicone/Nickel Nanostrand Nanocomposites." *Metallurgical and Materials Transactions A.* 42(2011): 3898-3906.
- 22. Koecher M. C. "Evaluation of Advanced Conductive Nickel Materials for Strain Sensing in Carbon Fiber Reinforced Polymers." (2012).
- 23. Oliver K. Johnson C. J. G., David T. Fullwood, & Brent L. Adams, N. H. a. G. H. "The Colossal Piezoresistive Effect in Nickel Nanostrand Polymer Composites and a Quantum Tunneling Model." *CMC*. 15(2010): 87-111.
- 24. Daniel Hernandez-Lobato J. M. H.-L., Amar Shah, Ryan P. Adams. "Predictive Entropy Search for Multi-Objective Bayesian Optimization." *JMLR*. 48(2016).
- 25. Jasper Snoek H. L. "Practical Bayesian Optimization of Machine Learning Algorithms."
- 26. Sam D. Tajbakhsh E. d. C., James L. Rosenberger. "A Fully Bayesian Approach to the Efficient Global Optimization Algoriothm." (2012).
- 27. Galuzio P. P., de Vasconcelos Segundo, E. H., Coelho, L. d. S., & Mariani, V. C. "Mobopt Multi-Objective Bayesian Optimization." *SoftwareX*. 12(2020).
- 28. Eric Brochu V. M. C., Nando de Freitas. "A Tutorial on Bayesian Optimization of Expensive Cost Functions, with Application to Active User Modeling and Hierarchical Reinforcement Learning." (2010).